

Passive Cooling Strategy for Reducing Load in a Building with an Integrated PCM on the Rooftop

Amirhossein Khayyaminejad¹, Amir Fartaj¹

¹ Department of Mechanical, Automotive, and Materials Engineering/University of Windsor
401 Sunset Ave, Windsor, Ontario, Canada
khayyam@uwindsor.ca; fartaj@uwindsor.ca

Abstract – Increasing energy consumption is a critical worldwide challenge. Based on the gathered data, heating, ventilation, and air conditioning systems in residential sectors consume 40% of the provided energy, primarily from non-renewable sources. To overcome this challenge, scientists are actively working to reduce reliance on fossil fuels by adopting renewable energy resources. In this research article, the thermal performance of a natural ventilation system within a building in Las Vegas by implementing phase change material during the hottest day of summer is investigated. The city of Las Vegas is selected because of its hot and arid climate. This system includes a solar chimney, an earth-to-air heat exchanger, and phase change material. This system is simulated in ANSYS Fluent software, and the RNG $k - \epsilon$ is selected as the turbulence model. The n-Henicosane is chosen as a phase change material to evaluate its impact on the cooling load when placed on the roof. Furthermore, the effect of phase change material layer thickness on the thermal performance of the natural cooling system is studied. The natural ventilation system reduces the peak indoor temperature by 15.5 K and saves 28.19 kW of energy during the day. Based on the simulations, the optimum thickness obtained is 70 mm. After integrating phase change material with this thickness in the building, the maximum indoor temperature is further reduced by 2.5 K to reach 298.5 K. This system at the peak load cuts 81% of the energy consumption and saves 33.21 kW in 24 hours. In conclusion, incorporating PCM into a building rooftop with a natural ventilation system is a prudent option in reducing the indoor temperature and energy demand in a hot and arid climate.

Keywords: PCM; Solar Chimney; Natural Ventilation; CFD; Earth-Air Heat Exchanger; Roof; Renewable Energy

1. Introduction

Worldwide energy consumption has been on the rise as populations continue to grow and economies develop. Electricity plays a crucial role in meeting the energy demands of modern society. However, the majority of electricity production still relies on oil, and natural gas, which contribute significantly to greenhouse gas emissions and climate change. By transitioning to renewable energy, it is possible to reduce dependence on non-renewable resources, mitigate the effects of climate change, and create a more sustainable future for generations to come. Renewable energy sources now account for over 29% of global electricity generation, according to the IEA [1]. The use of renewable energy resources is projected to continue to grow in the coming years, with the IEA forecasting that renewable electricity generation will increase by 50% between 2020 and 2025, driven by solar and wind power [1].

Renewable energy can be used in several ways in Heating, Ventilation, and Air-Conditioning (HVAC) systems. Employing renewable energy in HVAC systems results in improving indoor air quality (IAQ) and indoor thermal conditions. By improving energy efficiency and reducing reliance on fossil fuels, HVAC systems powered by renewable energy can create healthier and more comfortable living and working environments, while also promoting sustainability and reducing the environmental impact of buildings.

Phase Change Materials (PCMs) have been applied in residential and commercial sectors and roofs to regulate indoor temperature and reduce the energy consumption of HVAC systems. PCMs are a low-cost, low-maintenance solution for reducing energy consumption and increasing sustainability [2]. PCMs can be used to reduce the heat gain from the sun, which can help to lower the temperature inside the building. The PCM is typically encapsulated in a container or panel, then installed on top of the roof. As the sun heats the roof, the PCM absorbs the heat, preventing it from entering the building and keeping the indoor temperature cooler [3]. By implementing PCMs on the roof, the cooling load decreases because radiation heat transfer between the roof and the sun is more than in other parts of the buildings [4].

Many researchers studied the effect of PCM on buildings in recent years. The inner surfaces of the walls and roof are chosen to study their temperature distribution [5,6] and heat transfer [7,8]. Li et al. [5] focused on the effect of using PCM

on heat transfer through different roofs in a cold climate. They concluded that the PCM-integrated roofs strongly impacted the inner ceiling surface temperature. Moreover, the hottest indoor temperature was delayed beyond three hours compared with the non-PCM integrated roof. Pasupathy and Velraj [6] conducted a study to examine the thermal performance of a roof containing a phase change material (PCM) layer in a hot climate in India. Tokuç et al. [7] worked on PCM-integrated roofs experimentally and numerically. They claimed that the optimum PCM layer thickness is 20 mm for buildings in mediterranean climate. Alqallaf and Alawadh [9] conducted an experiment to examine a roof design comprising a concrete slab with cylindrical holes containing phase change material (PCM). They observed a reduction in heat flux at the indoor surface of the roof, up to 17%. Servando et al. [10] designed a new roof structure where PCM is encapsulated and fills the cavity of a hollow core slab. This innovative approach enhances the efficiency of cooling energy storage by utilizing ventilation during nighttime.

A solar chimney (SC), also known as a thermal chimney or solar updraft tower, is a passive solar ventilation system that utilizes the sun's energy to create airflow [11]. Solar chimneys can be used for passive cooling and ventilation in residential and commercial buildings. They offer a sustainable and energy-efficient alternative to conventional mechanical ventilation systems, as they rely solely on the sun's energy for operation [12]. Rabani et al. [13] experimentally studied solar chimney performance in Yazd, Iran. They achieved a 7 to 14 degrees reduction in indoor temperature during 24 hours. Amer et al. [14] studied Solar chimneys performance experimentally in Egypt, and their results revealed 8.5 degrees of indoor temperature reduction.

Combining solar chimneys with geothermal air systems is a widely recognized approach for decreasing energy usage and enhancing natural ventilation systems. This method utilizes earth-air heat exchangers to harness the stored energy within the ground. These systems' economic and environmental advantages have made them highly favored among designers and researchers [15]. Maerefat and Haghghi [16] conducted theoretical research, including a solar chimney with an Earth-Air Heat Exchanger (EAHE) known as SC-EAHE. They determined that this SC-EAHE system is capable of effectively cooling and ventilating a room. Based on their findings, they designed a coupled system that could meet the thermal comfort requirements of the occupants. In study by Kalantar and Khayyamnejad [17], they studied an SC-EAHE. They introduced a new circular geometry for SC made out of glass with a fin in the center of SC. They simulated their system in Yazd, Iran, weather conditions for the hottest summer day. They optimized the natural ventilation performance and reported that their designed EAHE decreased air temperature by 18 K.

In this research article, the thermal performance of the SC-EAHE system [17] is investigated under Las Vegas weather conditions. Furthermore, the effectiveness of the PCM integrated roof on the natural ventilation and cooling performance is determined, and the effect of PCM layer thickness is studied by selecting four different thicknesses.

2. Problem statement

A single-story building is modeled, and the thermal performance of the natural ventilation system is investigated during summer in Las Vegas, with a cylindrical solar chimney on the rooftop and an EAHE buried in the soil under the building. This combination of the equipments is called natural ventilation system. The passive cooling and natural ventilation system is employed to provide thermal comfort conditions for residents in a building (6 m (length) × 4 m (width) × 3 m (height)). A three-directional vertical fin which is made out of copper, has a common centreline with the chimney. This geometry of SC results in absorbing solar radiation in all directions (360°) and longer time during the day compared with Inclined solar chimnies. In addition, by using this three-dimensional fin, the absorption area is increased in comparison with traditional solar chimneys, which lead to higher efficacy of solar chimney.

EAHE is buried beneath the building. Hot airflow passes through the EAHE pipes, losing heat to the cool pipes buried in the soil. The length of the pipes allows the air to reach the minimum temperature. The air then flows upward, divided into four sections with registers located in the building's corners, improving air circulation. The temperature difference between the registers and the solar chimney outlet results buoyancy-driven flow (natural convection ventilation), with negative pressure at the EAHE inlet and positive pressure at the chimney outlet.

Fig.1 illustrates the simulated components. As it can be seen hot outdoor air is cooled in EAHE and then the cool air enters the building and after cooling the air, air flows into the solar chimney, then its temperature increases and then

flows out of the building. Based on their results [17] the SC height and diameter are 6 and 1 meters, respectively. The SC is equipped with 3 fins. Additionally, EAHE is buried at a depth of 7 meters, the EAHE's pipes have a diameter of 0.2 meters and a total length of 270 meters. Previous investigations have revealed that Las Vegas experiences desirable soil temperatures at a depth of 4 meters [18]. Since PCM is utilized to improve the natural system efficiency, it is expected that by implementing PCM on the roof, peak cooling load will decrease [3] and room temperature will be more stable [4] due to the latent heat gain. In addition, using PCM helps to reduce the heat transfer through building envelope, which in turn delays indoor temperature rise.

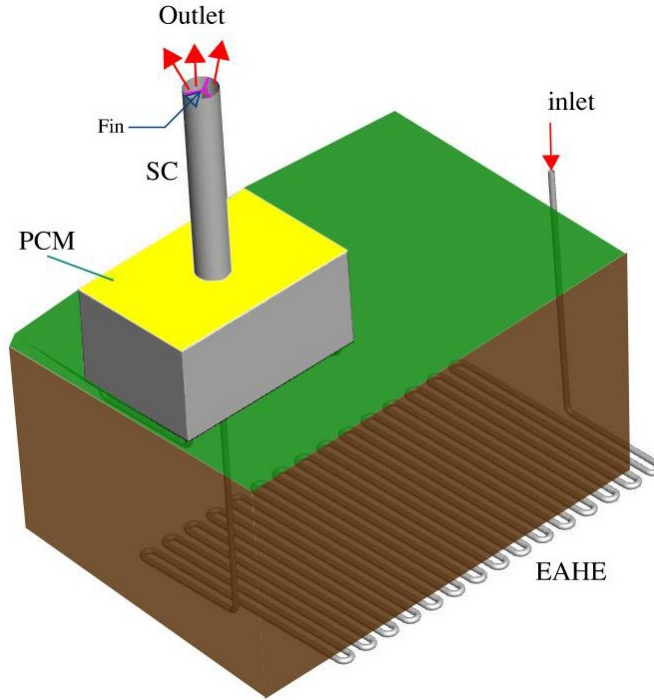


Fig. 1: Simulated natural cooling system

3. Numerical modelling

ANSYS Fluent 2022 R1 is employed to simulate the model using Computational Fluid Dynamic (CFD) equations and Finite Volume Method (FVM). A transient pressure-based type of solver is preferred with a SIMPLE algorithm approach to solve Pressure-Velocity equations. The selected time step is 90 seconds. Boussinesq Model calculates air density. Furthermore, the Solidification and melting features are activated. The ANSYS Meshing module is utilized to produce an unstructured tetrahedral network. Meshing is done by setting characteristics like growth rate (1.05) and the cell size range (0.05 -50 mm).

Fluid flow is assumed to be three-dimensional, unsteady, and incompressible. RANS (Reynolds Averaged Navier–Stokes) Numerical method is used to solve the fluid flow equations. Governing equations are Continuity, mass conservation (Eq. (1)) and, the conservation of momentum (Eq. (2)), energy conservation (Eq. (3)) equations are given below.

$$\frac{\partial \rho}{\partial t} + \nabla \cdot (\rho \vec{V}) = 0 \quad (1)$$

$$\rho \frac{\partial \vec{V}}{\partial t} + \rho (\nabla \cdot \vec{V}) \vec{V} = -\nabla P + \mu (\nabla^2 \vec{V}) + \rho_{ref} \beta (T - T_{ref}) \vec{g} \quad (2)$$

$$\frac{\partial (\rho H)}{\partial t} + \nabla (\rho H \vec{V}) = \nabla (k \nabla T) \quad (3)$$

Where ρ represents fluid density, V , T and P indicate fluid velocity, Temperature and pressure, respectively. Also H , μ , g and t defined as enthalpy, Fluid viscosity, gravitational accelerate and time, respectively. Moreover, β is the fluid thermal expansion

coefficient. To calculate the overall heat transfer through the PCM is given in Eq. (4), and sensible heat $Q_{sensible}$ (Eq. (5)) for PCMs calculate based on enthalpy.

$$Q_{total} = Q_{sensible} + Q_{latent} \quad (4)$$

$$Q_{sensible} = \int_{T_0}^T C_p dT + h_0 \quad (5)$$

Where C_p indicates fluid specific heat. The latent heat portion is calculated based on Eq. (6). Besides, in Eq. (7), θ represents the liquid fraction, while Γ denotes the latent heat of PCM. The fraction of liquid can be changed from “0” to “1” to obtain from [19]:

$$Q_{latent} = \theta \Gamma \quad (6)$$

$$\theta = \left\{ \begin{array}{ll} 0 & ; T < T_{solidus} \\ \frac{T - T_{solidus}}{T_{liquidus} - T_{solidus}} & ; T_{liquidus} < T < T_{solidus} \\ 1 & ; T_{liquidus} < T \end{array} \right\} \quad (7)$$

The RNG $k - \varepsilon$ turbulence model (Eqs. (8) – (9)) is based on the normalization group method applied to the conservation equation. Its advantage compared to other models is containing R_ε , to predict fluid flow behavior more accurately [20]. The R_ε is given as (Eq. (10)) Where $\eta \equiv \frac{S_k}{\varepsilon}$, $\eta_0 = 4.38$, $\beta = 0.012$. G_k and G_b indicate the production of turbulence kinetic energy based on mean velocity gradients, and buoyancy, respectively [21]. Prandtl numbers for k and ε are defined as α_k and α_ε . Source terms for k and ε are set by the user based on the boundary conditions. Y_M represents the fluctuations in turbulence over dissipation rate.

$$\frac{\partial}{\partial t}(\rho k) + \frac{\partial}{\partial x_i}(\rho k u_i) = \frac{\partial}{\partial x_j} \left(\frac{\alpha_k \mu_{eff} \partial k}{\partial x_j} \right) + G_k + G_b - \rho \varepsilon - Y_M + S_k \quad (8)$$

$$\frac{\partial}{\partial t}(\rho \varepsilon) + \frac{\partial}{\partial x_i}(\rho \varepsilon u_i) = \frac{\partial}{\partial x_j} \left(\frac{\alpha_\varepsilon \mu_{eff} \partial \varepsilon}{\partial x_j} \right) + C_{1\varepsilon} \frac{\varepsilon}{k} (G_k + C_{3\varepsilon} G_b) - C_{2\varepsilon} \rho \frac{\varepsilon^2}{k} - R_\varepsilon + S_\varepsilon \quad (9)$$

$$R_\varepsilon = \frac{\left(C_\mu \rho \eta^3 \left(1 - \frac{\eta}{\eta_0} \right) \right) \varepsilon^2}{1 + \beta \eta^3} \frac{1}{k} \quad (10)$$

4. Boundary Conditions

This simulation is done based on Las Vegas Weather data on July 1st, which is the hottest day in the year. Based on the literature [18] the assumed ambient temperature in simulation differs during hours of the day. The desired indoor temperature falls within the range of 293.15 K to 299.15 K. To simulate solar load, a ray-tracing solar load model is employed. The latitude and longitude coordinates of Las Vegas, Nevada, United States, are 36.1699° N and -115.1398° W. Las Vegas elevation is 610 m above sea level and the operating pressure. Ambient and soil temperature are imported to ANSYS FLUENT by User Defined Functions (UDF)[16,18]. PCM is selected based on the working condition. The best PCM in this application is the one with having similar melting point to the peak load temperature [3,19].

The selected PCM is n-Henicosane (C_{21}) with melting point of 314.15 K, solidification point of 312.15 K, latent heat of 210 kJ/kg, and thermal conductivity of 0.2 W/mK [19]. Thermal expansion coefficient for air is assumed $0.0034 \frac{1}{K}$. EAHE pipes are made of clay, and their thickness is 0.015 m. R-22 is selected as Building wall insulation. The solar chimney includes 10 mm clean glass and assumed as semi-transparent. Fin's thermal boundary conditions are selected as coupled. In this simulation, all components participate in the solar load calculation model except EAHE.

5.1. Mesh Independency

The grid independency approach aims to determine the optimal cell number for accurate simulation while keeping computational costs in check. In this phase, the geometry is examined with six different cell numbers (from 752,736 to 5,683,423) to identify a suitable cell count. Based on the simulations, results converged for geometries more than 2,767,896 cell number. There was a 0.075% difference in average indoor temperature between 2,767,896 cells and 4,183,355 cells. Therefore, the mesh network with 2,767,896 cells is taken into consideration for further simulation.

5.2. Validation

Maytorena et.al [3] analyzed thermal performance of an EAHE for cooling a room in Mexican desert climate. They simulated their model by Ansys Fluent and verified their simulation with an experimental model. In addition, Maytorena et.al [3] used PCM on the roof to enhance their system performance. In the current paper, numerical study of Maytorena et.al [3] is simulated to verify the accuracy of the numerical simulation and mathematical model. Fig. 2 shows temperature of ceiling of the room with PCM in current study and Maytorena et.al [3]. Results are in a good agreement and the maximum error is 1.4% which is occurred at the time of 14:15.

6. Results and Discussion

In this part, two sections of the simulation will be discussed. The first one is simulation of the natural ventilation system in Las Vegas and the second one the effect of PCM's thickness is studied.

6.1. System Performance in Las Vegas, USA

The passive ventilation and cooling system is simulated in Las Vegas, USA. The average indoor and ambient temperatures are given in Fig. 3. The disparity between ambient and indoor temperatures can indicate the effectiveness of the SC-EAHE system. This parameter is variable between 1.8 and 15.5 K. The passive cooling system is more effective in hot hours of the day when the temperature difference between ambient and indoor is between 6 and 15.5 K. In other words, the passive cooling system plays an important role when the outdoor temperature and cooling load are higher. The SC-EAHE system maintains the indoor temperature between 298.5 and 330.5 K. Another parameter that can be analyzed is the temperature fluctuation over 24 hours. The indoor temperature range throughout the day is 2.5 K.

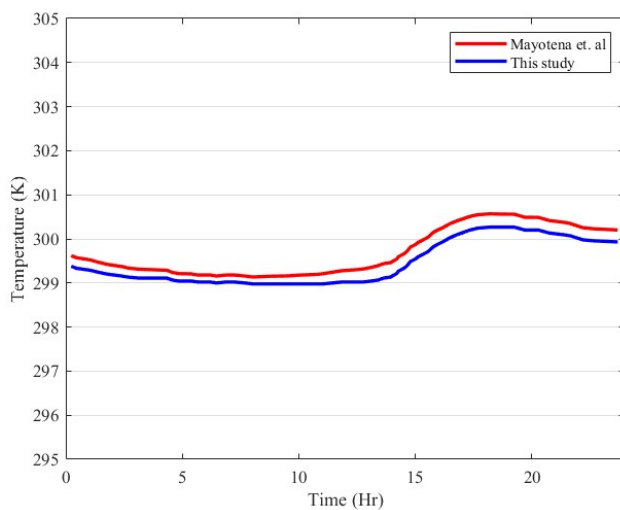


Fig. 2: ceiling temperature during 24 hours based on [4].

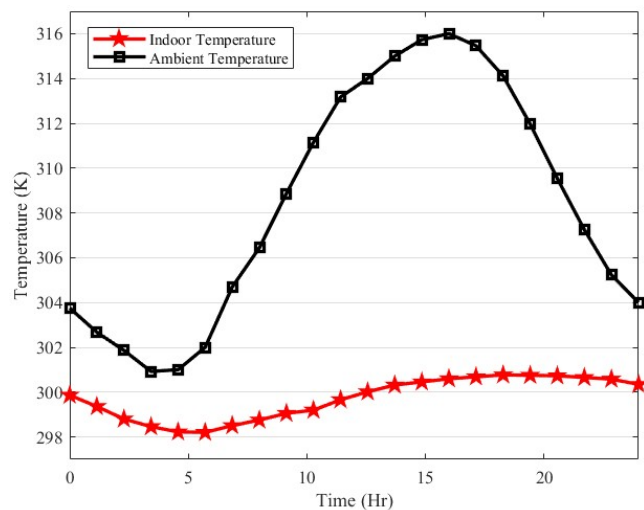


Fig. 3: Ambient and Indoor temperature graph during simulation.

6.2. Effect of PCM thickness

Four different thicknesses (30 mm, 50 mm, 70 mm, and 90 mm) are selected to investigate the effect of PCM layer thickness. Fig. 4 shows the hourly indoor temperature for different thicknesses. The effectiveness of the PCM layer on system's thermal performance is more sensible in hot hours of the day. The average indoor temperature is warmer when PCM layer is 30 mm thick. By increasing PCM thickness, the indoor temperature experienced cooler conditions until 90 mm. The difference in Indoor maximum temperature between 70 mm and 90 mm is 0.05% which means that by adding 20 mm of PCM when the PCM thickness is already 70 mm, the indoor temperature will remain constant. By increasing thickness from 30 mm to 70 mm, the peak indoor temperature is reduced 0.6 K. By adding a PCM layer with 70 mm thickness. Also, the temperature range is 2.5 K without PCM, while this parameter reaches 0.8 K after using PCM.

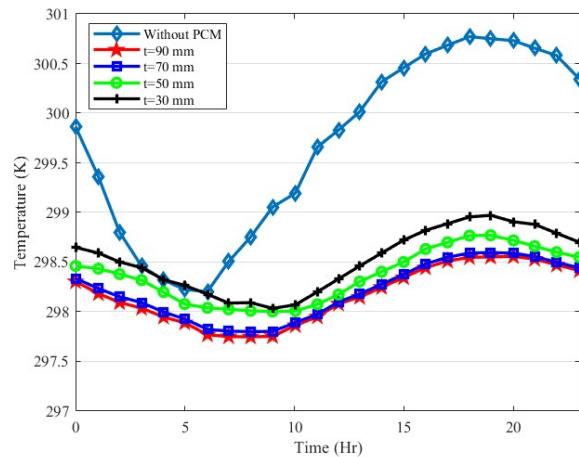


Fig. 4: Indoor temperature during simulation for different thicknesses of PCM.

6.3. Energy Saving

Fig.5 shows the hourly temperature of Ambient temperature, the indoor temperature in the presence of SC-EAHE, and the indoor temperature by using SC-EAHE with PCM. For the hottest hour of the day, SC-EAHE reduces Indoor temperature to 300.5 K, and by using SC-EAHE, the indoor temperature reaches 298.5 K. Furthermore, using PCM is more effective during the time that the building is experiencing the peak load. Peak load is the highest amount of demanded cooling to maintain the indoor air in the comfort zone. Fig. 5 illustrates the Hourly cooling load of the building and the amount of supported cooling load by the passive cooling system. The peak load is 3.15 kW at 15:30. At the same time, SC-EAHE saves up to 2.25 kW and supports 71% of the cooling load. By integrating PCM, the passive cooling system saves up to 2.56 kW and provides 81% of the cooling load. SC-EAHE system saves 28.19 kW during 24 hours, while by adding PCM, saved energy increases to 33.21 kW.

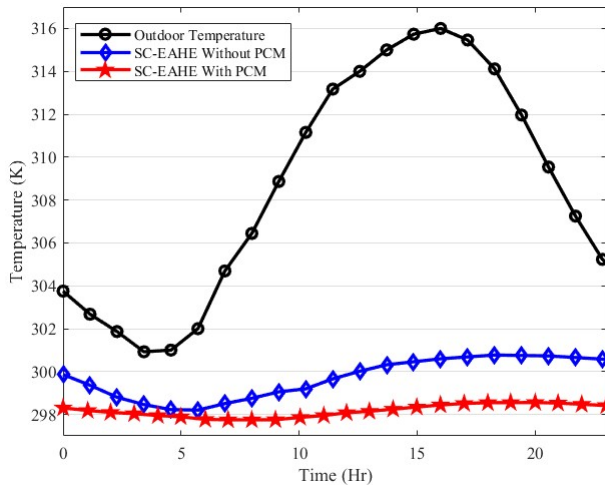


Fig. 5: Hourly outdoor and indoor temperature.

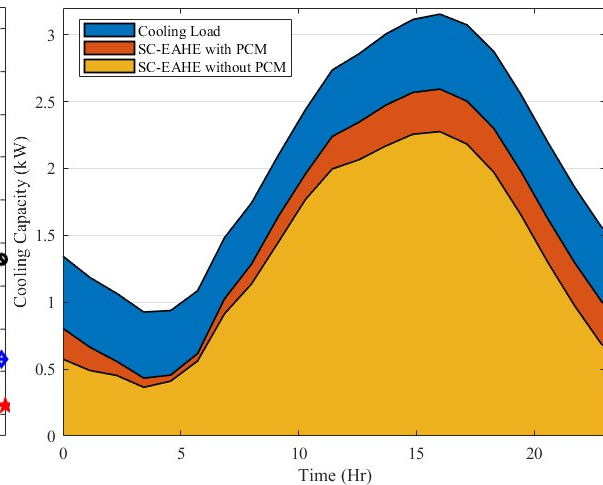


Fig. 6: Hourly building cooling load and cooling capacity of passive cooling system.

7. Conclusion

The thermal performance of a natural ventilation and cooling system on the hottest day of summer in Las Vegas is investigated. The result showed that the system could decrease building indoor temperature by up to 15.5 K and the cooling load by 71% at the peak ambient temperature. It is worth mentioning that 28.19 kW of energy consumption saved during the entire day. The integration of PCM on the rooftop, along with the SC-EAHE system, further reduced the indoor temperature by 2.5 K at the peak ambient temperature, and the cooling load by 33.21 kW for entire day. Hence, using the passive ventilation and cooling system decreases the air conditioning system's workload, resulting in lower maintenance and utility costs. The system's ability to significantly reduce indoor temperature, cooling load, and energy consumption enhances occupant thermal comfort and contributes to environmental sustainability by reducing reliance on conventional air conditioning systems. These findings have practical implications for architects, engineers, and policymakers in designing and implementing energy-efficient and sustainable cooling strategies for buildings in similar climates.

References

- [1] "Renewables 2021 dataset - Data product - IEA," IEA. <https://www.iea.org/data-and-statistics/data-product/renewables-2021-dataset>.
- [2] M. Momeni, S. Askar, and A. Fartaj, 'Thermal performance evaluation of a compact two-fluid finned heat exchanger integrated with cold latent heat energy storage', *Appl. Therm. Eng.*, vol. 230, no. 120815, p. 120815, Jul. 2023.
- [3] V. M. Maytorena, J. F. Hinojosa, S. Moreno, and D. A. Buentello-Montoya, *Thermal performance analysis of a passive hybrid earth-to-air heat exchanger for cooling rooms at Mexican desert climate. Case Studies in Thermal Engineering*, 2023.
- [4] K. W. Shah, P. J. Ong, M. H. Chua, S. H. G. Toh, J. J. C. Lee, X. Y. D. Soo, Z. M. Png, R. Ji, J. Xu, and Q. Zhou, 'Application of phase change materials in building components and the use of nanotechnology for its improvement', *Energy Build.*, vol. 262, no. 112018, p. 112018, May 2022.
- [5] D. Li, Y. Zheng, C. Liu, and G. Wu, 'Numerical analysis on thermal performance of roof contained PCM of a single residential building', *Energy Convers. Manag.*, vol. 100, pp. 147–156, Aug. 2015.
- [6] A. Pasupathy and R. Velraj, 'Effect of double layer phase change material in building roof for year round thermal management', *Energy Build.*, vol. 40, no. 3, pp. 193–203, 2008.

- [7] A. Tokuç, T. Başaran, and S. C. Yesügey, ‘An experimental and numerical investigation on the use of phase change materials in building elements: The case of a flat roof in Istanbul’, *Energy Build.*, vol. 102, pp. 91–104, Sep. 2015.
- [8] X. Jin and X. Zhang, “Thermal analysis of a double layer phase change material floor,” *Applied Thermal Engineering*, vol. 31, no. 10, pp. 1576–1581, Jul. 2011, doi: 10.1016/j.applthermaleng.2011.01.023.
- [9] H. J. Alqallaf and E. M. Alawadhi, ‘Concrete roof with cylindrical holes containing PCM to reduce the heat gain’, *Energy Build.*, vol. 61, pp. 73–80, Jun. 2013.
- [10] S. Alvarez, L. F. Cabeza, A. Ruiz-Pardo, A. Castell, and J. A. Tenorio, ‘Building integration of PCM for natural cooling of buildings’, *Appl. Energy*, vol. 109, pp. 514–522, Sep. 2013.
- [11] M. S. B. Jahromi, V. Kalantar, H. S. Akhijahani, H. Kargarsharifabad, and S. Shoeibi, ‘Performance analysis of a new solar air ventilator with phase change material: Numerical simulation, techno-economic and environmental analysis’, *Journal of Energy Storage*, vol. 62, 2023.
- [12] S. Jafari and V. Kalantar, ‘Numerical simulation of natural ventilation with passive cooling by diagonal solar chimneys and windcatcher and water spray system in a hot and dry climate’, *Energy Build.*, vol. 256, no. 111714, p. 111714, Feb. 2022.
- [13] R. Rabani, A. K. Faghieh, M. Rabani, and M. Rabani, ‘Numerical simulation of an innovated building cooling system with combination of solar chimney and water spraying system’, *Heat Mass Transf.*, vol. 50, no. 11, pp. 1609–1625, Nov. 2014.
- [14] E. H. Amer, “Passive options for solar cooling of buildings in arid areas,” *Energy*, vol. 31, no. 8–9, pp. 1332–1344, Jul. 2006, doi: 10.1016/j.energy.2005.06.002.
- [15] R. Elghamry and H. Hassan, “An experimental work on the impact of new combinations of solar chimney, photovoltaic and geothermal air tube on building cooling and ventilation,” *Solar Energy*, vol. 205, pp. 142–153, Jul. 2020, doi: 10.1016/j.solener.2020.05.049.
- [16] M. Maerefat and A. P. Haghighi, ‘Passive cooling of buildings by using integrated earth to air heat exchanger and solar chimney’, *Renew. Energy*, vol. 35, no. 10, pp. 2316–2324, Oct. 2010.
- [17] V. Kalantar and A. Khayyaminejad, ‘Numerical simulation of a combination of a new solar ventilator and geothermal heat exchanger for natural ventilation and space cooling’, *Int. J. Energy Environ. Eng.*, vol. 13, no. 2, pp. 785–804, Jun. 2022.
- [18] R. Vidhi, “A Review of Underground Soil and Night Sky as Passive Heat Sink: Design Configurations and Models,” *Energies*, vol. 11, no. 11, p. 2941, Oct. 2018, doi: 10.3390/en11112941.
- [19] M. Momeni and A. Fartaj, ‘Numerical thermal performance analysis of a PCM-to-air and liquid heat exchanger implementing latent heat thermal energy storage’, *J. Energy Storage*, vol. 58, no. 106363, p. 106363, Feb. 2023.
- [20] T. Tsumura, T. Kunihiro, and K. Ohnishi, “Derivation of covariant dissipative fluid dynamics in the renormalization-group method,” *Physics Letters B*, vol. 646, no. 2–3, pp. 134–140, Mar. 2007, doi: 10.1016/j.physletb.2006.12.074.
- [21] A. Khayyaminejad, N. P. Khabazi, F. Gholami-Malek Abad, and S. Taheripour, (2023). Numerical Investigation on the Effect of the Geometric Parameters of the Impeller on Vortex Pump Performance. *Iranian Journal of Science and Technology, Transactions of Mechanical Engineering*, 1-21.